From p- to n-Type Mixed Conduction in Isoindigo-Based Polymers through Molecular Design

Dedicated to the memory of Jorge Borges-González

*Zachary S. Parr, Jorge Borges-González, Reem B. Rashid, Karl J. Thorley, Dilara Meli, Bryan D. Paulsen, Joseph Strzalka, Jonathan Rivnay and Christian B. Nielsen**

Dr. Z. S. Parr, Dr. J. Borges-González, Dr. C. B. Nielsen
Department of Chemistry, Queen Mary University of London, Mile End Road, London E1 4NS, UK
E-mail: c.b.nielsen@qmul.ac.uk

R. B. Rashid, Dr. B. D. Paulsen, Prof. J. Rivnay
Department of Biomedical Engineering, Northwestern University, 2145 Sheridan Road, Evanston, IL 60208, USA

D. Meli
Department of Materials Science and Engineering, Northwestern University, 2145 Sheridan Road, Evanston, IL 60208, USA

Prof. J. Rivnay
Simpson Querrey Institute, Northwestern University, Chicago, IL 60611

Dr. J. Strzalka
X-Ray Science Division, Argonne National Laboratory, Lemont, IL 60439, USA

Dr. K. J. Thorley
Center for Applied Energy Research, University of Kentucky, Lexington KY 40511, USA

Keywords: organic bioelectronics, mixed conductors, semiconducting polymers, isoindigo, donor-acceptor polymers

Organic mixed ionic and electronic conductors are of significant interest for bioelectronic applications. Here, we use three different isoindigoid building blocks to obtain polymeric mixed conductors with vastly different structural and electronic properties which can be further fine-tuned through the choice of comonomer unit. We show how careful design of the isoindigoid scaffold can afford highly planar polymer structures with high degrees of electronic delocalization, while subtle structural modifications can control the dominant charge carrier (hole or electron) when probed in organic electrochemical transistors. We employ a combination of experimental and computational techniques to probe electrochemical, structural and mixed ionic and electronic properties of the polymer series

which in turn allows us to derive important structure-property relations for this promising class of materials in the context of organic bioelectronics. Ultimately, we use these findings to outline robust molecular design strategies for isoindigo-based mixed conductors that can support efficient p-type, n-type and ambipolar transistor operation in an aqueous environment.

1. Introduction

With the growing interest in organic bioelectronics, organic mixed ionic and electronic conductors (OMIECs) are gaining significant attention.[1–3] While the field has been largely dominated by poly(3,4-ethylenedioxythiophene) polystyrene sulfonate (PEDOT:PSS) and closely related derivatives as the active material,[4–7] new semiconducting materials have started to enter the arena in recent years.[8–12] In particular hole-transporting (p-type) mixed conductors have emerged with properties on par or even better than benchmark PEDOT:PSS formulations,[9,13,14] whereas electron-transporting (n-type) materials are still lacking considerably in terms of mixed conduction performance.[15–19]

The design of semiconducting materials for bioelectronic applications is heavily influenced by the rich body of literature in the broader field of organic electronics, evidenced by the development of e.g. oligo- and polythiophenes,[8,11,20,21] fullerenes,[18] diketopyrrolopyrrole-,[12,22–24] and naphthalene diimide-based[15,16] systems as efficient OMIECs. With that in mind, another versatile and highly efficient charge transporting moiety, isoindigo, has received very little attention for bioelectronic applications.[25] The isoindigo motif depicted in Figure 1a can be structurally modified not only by introducing various solubilizing chains through *N*-alkylation and substituents such as fluorine and chlorine on the aromatic rings but also by using different peripheral aromatic rings than benzene such as pyridine and thiophene.[26–28] The choice of peripheral aromatic unit can have a pronounced effect on the electron-rich or –deficient character of the isoindigoid building block and consequently on the frontier energy levels of the resulting isoindigoid materials through push-

pull type electronic interactions with the chosen coupling partner when constructing extended π-conjugated systems. Electronic interactions along the π-conjugated system are also affected by the degree of planarity of the molecular scaffold and consequently by potential steric interactions both within the isoindigoid moiety itself and between neighboring units along the π-conjugated system. Notably, whereas the dihedral angle ϕ_1 (see Figure 1a) between the two isatin moieties in the parent isoindigo is found experimentally to be around 22° and calculated to be around 16°,[29,30] 7,7'-diazaisoindigo benefits from a completely coplanar conformation (ϕ_1 = 0°) as probed by density functional theory (DFT) and verified experimentally from single crystal structure determination.[28,30] A finding which is ascribed to the shorter C-N bond in the pyridine motif and consequently less steric repulsion between the lactam oxygen and the aryl hydrogen. Moreover, when considering ϕ_2, referring to the dihedral angle between the isoindigoid motif and an adjacent thiophene unit (chosen as an example as this is a highly prevalent comonomer), the 7,7'-diazaisoindigo again offers a more coplanar linkage with adjacent aromatic units than isoindigo itself as indicated in Figure 1a. The adjacent thiophene moiety can adapt two coplanar conformations favored by either an attractive S—N interaction (ϕ_2 = 0°) or by the lack of repulsive H—H interactions (ϕ_2 = 180°). The thienoisoindigo motif also displayed in Figure 1a is yet another structural modification where both ϕ_1 and ϕ_2 are around 0° in this case due to the lack of lactam oxygen and aryl hydrogen interactions (ϕ_1) and the s-trans configuration of the thiophene-thiophene linkages (ϕ_2).

Based on these considerations around polymer backbone planarity as well as the vastly different electronic properties of the isoindigo-derived building blocks discussed here, we have used the three motifs, isoindigo (IG), 7,7'-diazaisoindigo (AIG) and thienoisoindigo (TIG) to create a series of isoindigo-based copolymers. By copolymerization with electron-rich thiophene (T) and electron-deficient 2,1,3-benzothiadiazole (BT), the six copolymers depicted in Figure 1b were afforded. The lactam nitrogens were in all cases functionalized

with an amphipathic side chain comprising a five-methylene spacer and a terminal triethylene glycol segment to allow ion-diffusion within the bulk polymer film.[25,31] We have used this series of polymers to extract important structure-property relations in the context of mixed conduction, which in turn has enabled us to develop efficient p- and n-type OMIECs and outline future strategies for developing high-performing ambipolar OMIECs.

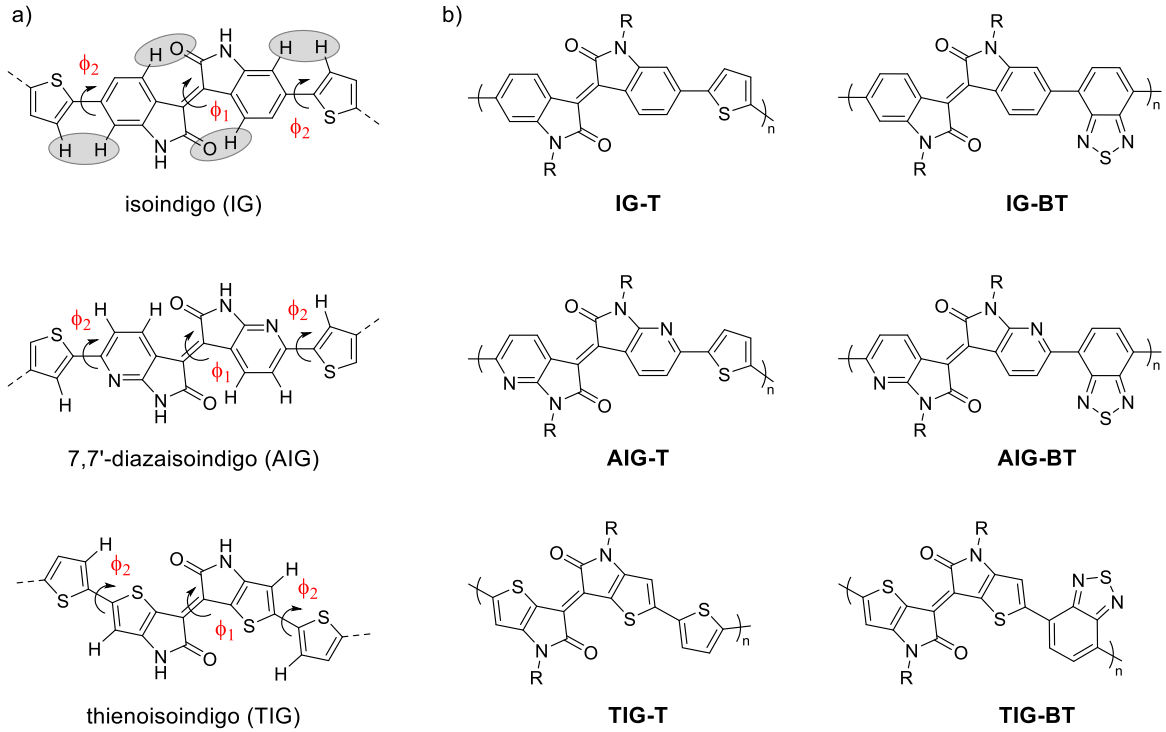

Figure 1. a) Isoindigo, 7,7'-diazaisoindigo and thienoisoindigo scaffolds with important dihedral angles (ϕ_1 and ϕ_2) and steric interactions (grey shading) highlighted. b) Synthesized isoindigo-, 7,7'-diazaisoindigo- and thienoisoindigo-based copolymers; in all cases R = $(CH_2)_5(OCH_2CH_2)_3OCH_3$.

2. Results and Discussion

2.1. Synthesis and Characterization

As further detailed in the Supporting Information, the polymers studied herein were synthesized using established synthetic methodologies by first constructing the isoindigo, 7,7'-diazaisoindigo and thienoisoindigo cores with amphipathic side chains comprising a five-methylene spacer and a terminal triethylene glycol segment.[28,32–34] Following bromination,

the reactive monomers were subject to Stille polycondensation with 2,5-bis(trimethylstannyl)-thiophene to afford thiophene copolymers **IG-T**, **AIG-T** and **TIG-T** and to Suzuki poly-condensation with 2,1,3-benzothiadiazole-4,7-bis(boronic acid pinacol ester) to afford 2,1,3-benzothiadiazole copolymers **IG-BT**, **AIG-BT** and **TIG-BT**. The crude polymers were purified by Soxhlet extractions, after which the polymers were obtained with estimated weight average molecular weights of 35 kDa, 29 kDa and 26 kDa for **IG-BT**, **AIG-T** and **AIG-BT**, respectively, as determined by gel permeation chromatography and further detailed in the SI. **IG-T** was found to have a lower weight average molecular weight of 13 kDa, while the molecular weights of **TIG-T** and **TIG-BT** could not be measured reliably due to polymer aggregation in solution, particularly at high concentrations needed for gel permeation chromatography, as also reported previously for related systems.[8,12] Matrix-assisted laser desorption ionization mass spectrometry confirmed degrees of polymerization up to at least ten for the two TIG polymers that could not be analyzed reliably with gel permeation chromatography (Figure S16). The polymers are moderately soluble in chlorinated solvents such as chloroform, chlorobenzene and 1,2-dichlorobenzene and show good thermal stability up to 350 °C (Figure S17).

2.2. Optical and Electrochemical Properties

The optical properties of the polymers in their solid state, as thin films spin-cast from chloroform solutions onto glass substrates, were investigated using absorption spectroscopy as depicted in Figure 2a. Among the thiophene copolymers, **AIG-T** is slightly red-shifted compared to **IG-T** with absorption maxima at 721 nm and 712 nm, respectively. **TIG-T**, on the other hand, owing to a much stronger push-pull effect, has its main absorption band in the NIR region with an absorption maximum at 1016 nm.[26] Weaker push-pull interactions are evident in the benzothiadiazole copolymers with **AIG-BT** and **TIG-BT** blue-shifted (absorption maxima at 674 nm and 994 nm, respectively) compared to their thiophene counterparts. **IG-BT** is markedly blue-shifted with an absorption maximum at 463 nm, which

is ascribed to significant backbone twisting due to the unfavorable phenyl-phenyl linkages (large ϕ_2 dihedral angle, Figure 1a) in this copolymer.

Electrochemical properties of the polymers in the solid state were elucidated using cyclic voltammetry on drop-cast films with 0.1 M aqueous NaCl as supporting electrolyte. As illustrated in Figure 2b, **TIG-T** showed clear and reversible oxidative behavior with a high current density response and good cycling stability; an onset of oxidation around 0.3 V against the Ag/Ag^+ redox couple was measured. In comparison, films of **IG-T** and **AIG-T** of similar thickness showed very limited electrochemical responses although a slight non-reversible oxidative event with an onset of oxidation around 0.95 V could be identified for **IG-T** (see Figure 2b, lower panel, left). For the benzothiadiazole copolymers, **TIG-BT** showed reversible and stable events both upon oxidation and reduction with onsets around 0.35 V and -0.8 V, respectively. Much lower current densities were again seen for the corresponding isoindigo and 7,7'-diazaisoindigo polymers, although a small Faradaic-like reductive event was observed for **AIG-BT** with no clear onset of reduction (Figure 2b, lower panel, right).

The ionization potentials (IPs) of the polymers were assessed by oxidative cyclic voltammetry on drop-cast films measured in acetonitrile-based electrolyte (Figure S18 and Table S1). **TIG-T** displayed the lowest IP around 4.5 eV, with **IG-T** (5.3 eV) and **AIG-T** (5.6 eV) having significantly higher IP values. In all cases, the BT copolymers had slightly larger IP values by around 0.2-0.3 eV compared to the corresponding thiophene copolymers. The electron affinities (EAs) were subsequently estimated from the IP values and the optical band gaps, with **AIG-BT** and **AIG-T** displaying high EA values of 4.2 eV and 4.0 eV, respectively, while **IG-BT** and **IG-T** had EAs of 3.7 eV and 3.8 eV, respectively. The more electron-rich TIG polymers still showed relatively high EA values of 3.9 eV for **TIG-BT** and 3.6 eV for **TIG-T** owing to their very narrow optical band gaps around 0.9 eV. These values are all in good agreement with previously published polymers with similar backbones.[26,28,35,36]

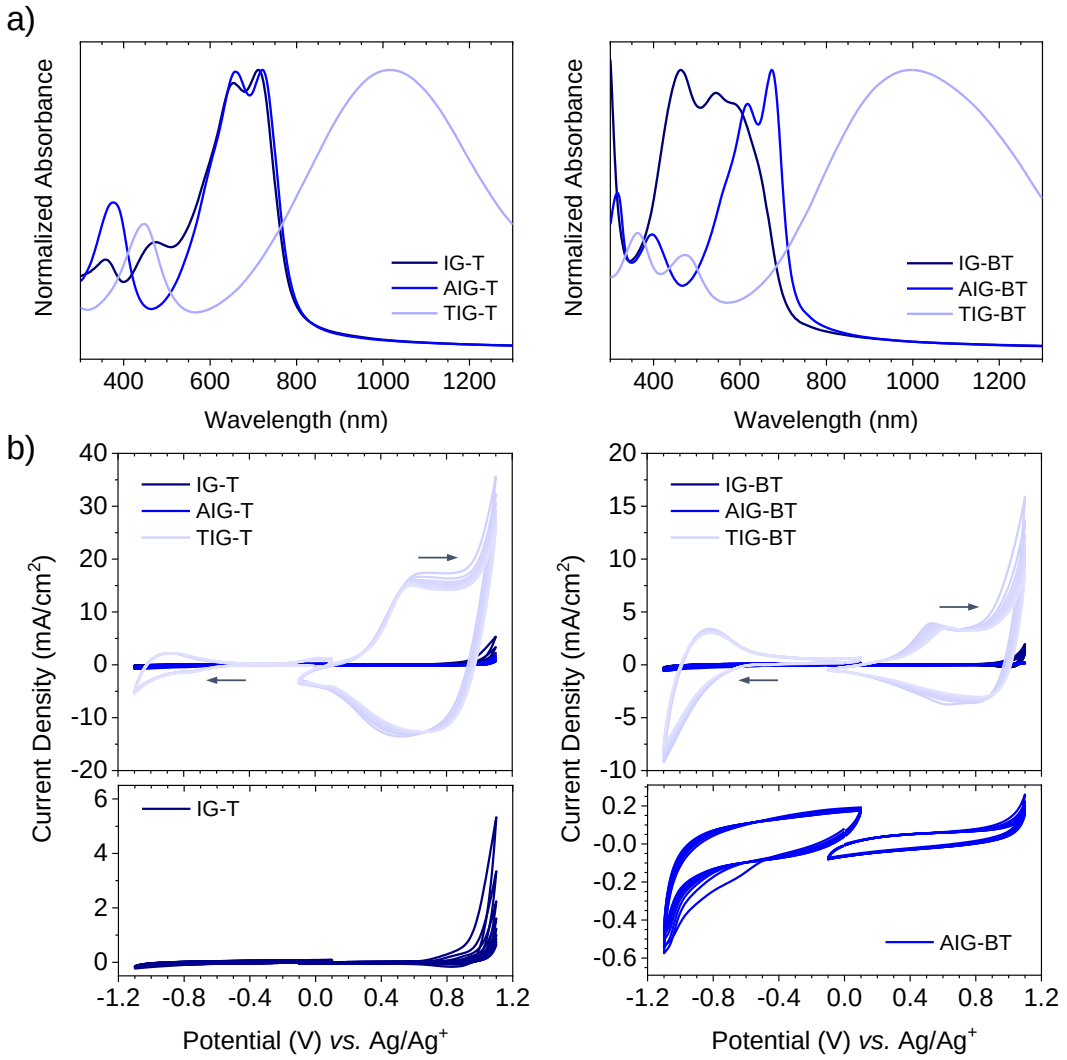

Figure 2. a) UV-Vis-NIR absorption spectra of thin films (spin-cast from 5 mg ml^{-1} chloroform solution onto glass substrate) of thiophene (left) and benzothiadiazole (right) copolymers. b) Cyclic voltammograms of thin films (drop-cast from 5 mg ml^{-1} chloroform solution onto glassy carbon electrode) of thiophene (left) and benzothiadiazole (right) copolymers recorded in 0.1 M aqueous NaCl solution at a scan rate of 100 mV s^{-1}; each polymer film cycled ten times with scan numbers 2-10 shown here; CV scan directions indicated by arrows.

Having identified the copolymers with significant electrochemical responses in aqueous electrolyte, we next investigated spectroelectrochemical properties (Figure 3 and Figure S20-S21), again by considering thin polymer films in aqueous electrolyte to mimic the operating conditions of relevant bioelectronic devices such as the organic electrochemical transistor. Among the thiophene copolymers, both **IG-T** and **TIG-T** showed complete bleaching of the neutral absorption bands (around 700 nm and 1000 nm, respectively) with

concurrent appearance of a positive polaron absorption band upon electrochemical oxidation as shown in Figure 3. For both polymers, nearly complete bleaching of the neutral absorption band happened within a narrow potential window of roughly 0.3 V (Figure 3b, left) with onsets of oxidation estimated at 0.8 V and 0.3 V for **IG-T** and **TIG-T**, respectively, which is in good agreement with the electrochemical data discussed above. Corroborating the irreversible nature of the electrochemical oxidation of **IG-T** in aqueous electrolyte, no clear and gradual increase in intensity of the polaronic absorption features with increasing potential was observed for **IG-T** (Figure 3a) which indicates rapid decomposition of the oxidized species during the experiment. The polaronic absorption band of **TIG-T** extends into the NIR region of the spectrum where the O-H stretching overtone dominates; repeating the experiment in acetonitrile solution, the positive polaron was found to have an absorption maximum at ~1900 nm (see Figure S19). For the benzothiadiazole-containing polymers, the observed electrochemical reductive (**AIG-BT**) and oxidative (**TIG-BT**) behavior was supported by the spectroelectrochemical studies, which showed bleaching of the neutral absorption bands (around 650 nm and 950 nm, respectively) and concurrent appearance of negative and positive polaronic absorption bands, respectively, as depicted in Figure 3a (right). Both benzothiadiazole polymers showed a slower and more gradual redox process spanning ~0.8 V for complete bleaching (Figure 3b, right); onsets were estimated at -0.5 V for **AIG-BT** (reduction) and 0.2 V for **TIG-BT** (oxidation). **AIG-BT** displayed a weak and broad negative polaron band with a maximum around 1040 nm, while the positive polaron absorption feature for **TIG-BT** had a maximum at ~1700 nm (determined in acetonitrile, Figure S19).

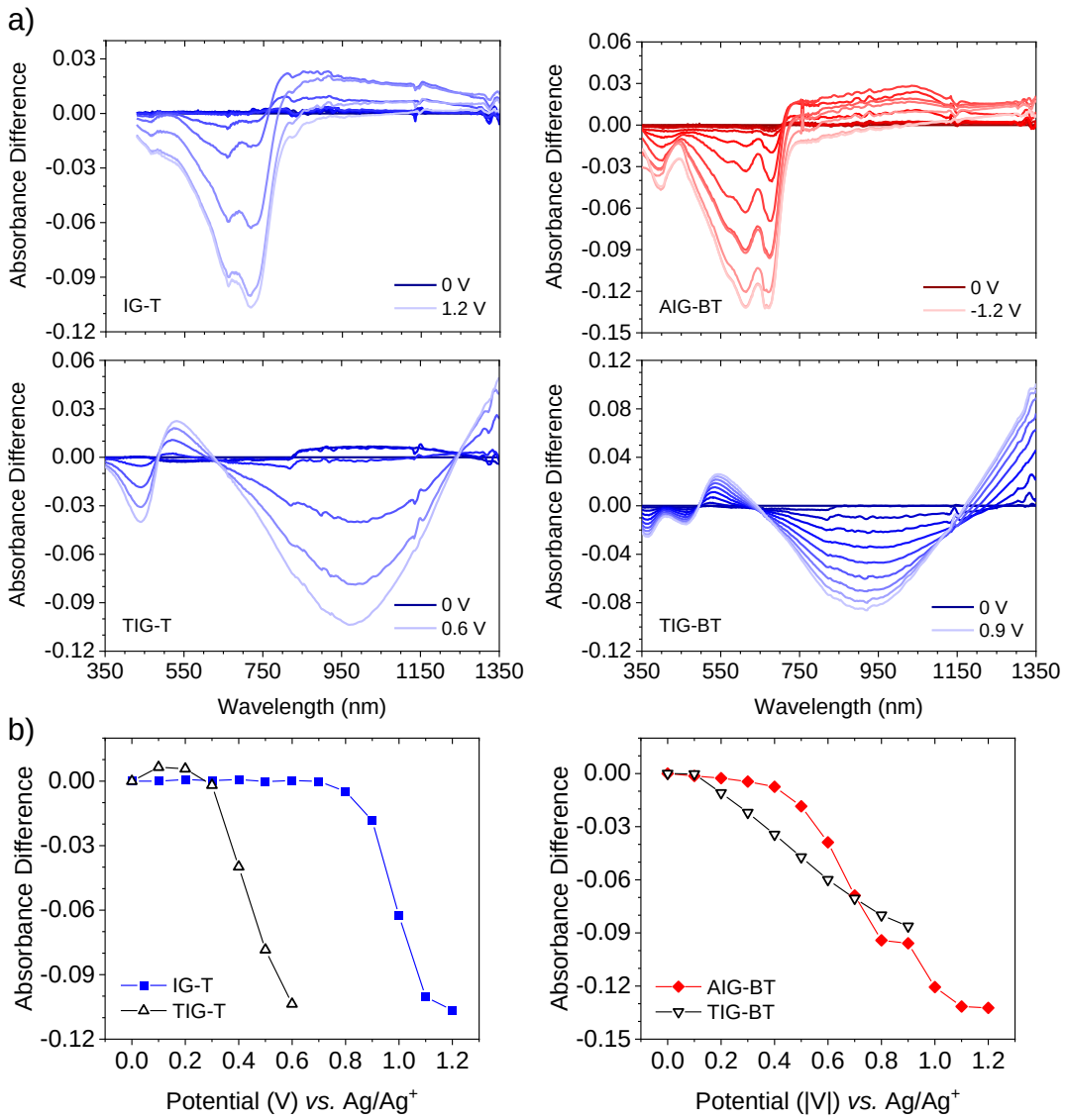

Figure 3. a) Spectroelectrochemistry of polymer films (spin-cast from 5 mg ml^{-1} chloroform solution onto ITO-coated glass substrate) of thiophene (left) and benzothiadiazole (right) copolymers recorded in 0.1 M aqueous NaCl solution with potential increments of 0.1 V. b) Bleaching (absorbance difference from 0 V spectrum) plotted as a function of applied potential for **IG-T** (recorded at 716 nm) and **TIG-T** (972 nm) (left) and **AIG-BT** (672 nm) and **TIG-BT** (920 nm) (right).

2.3. Transistor Characterization

In order to assess the mixed ionic and electronic conduction properties of the polymer series, organic electrochemical transistors (OECTs) were fabricated with drop-cast polymer active layers, aqueous NaCl electrolyte and a Ag/AgCl gate electrode. Corroborating the electrochemical and spectroelectrochemical studies in aqueous electrolyte, **IG-T**, **TIG-T**, and

TIG-BT showed p-type OECT operation whereas **AIG-BT** functioned as an n-type mixed conductor as evidenced in Figure 4, Figure S22 and Table 1. Of the p-type OMIECs, **IG-T** showed relatively poor device performance with μA currents and a normalized transconductance value of 23 mS cm^{-1}. The two thienoisoindigo polymers, on the other hand, performed significantly better with mA current responses and maximum transconductance values of 52 S cm^{-1} and 23 S cm^{-1}, respectively, for **TIG-T** and **TIG-BT**. In agreement with the observed electrochemical onsets of oxidation, the **TIG-T** based device turned on with a lower threshold voltage of -0.20 V compared to -0.34 V for **TIG-BT** while the maximum transconductance was likewise reached at a lower bias of -0.6 V for **TIG-T** compared to -0.75 V for **TIG-BT**. Considering the more electron-deficient **AIG-BT** polymer, with very high IP and EA values of 5.9 eV and 4.2 eV, respectively, OECT device characteristics confirmed the n-type behavior with a threshold voltage of 0.55 V and a maximum transconductance of 29 mS cm^{-1} observed at a gate voltage of 0.75 V. The isoindigo-based **IG-T**, which needed to be biased at a relatively high potential (-0.8 V), showed rapid deterioration of performance during OECT cycling tests (Figure S22), whereas **TIG-T**, **TIG-BT**, and **AIG-BT** showed very good operational stability with less than 10% loss of current response after 400-500 cycles as shown in Figure 4.

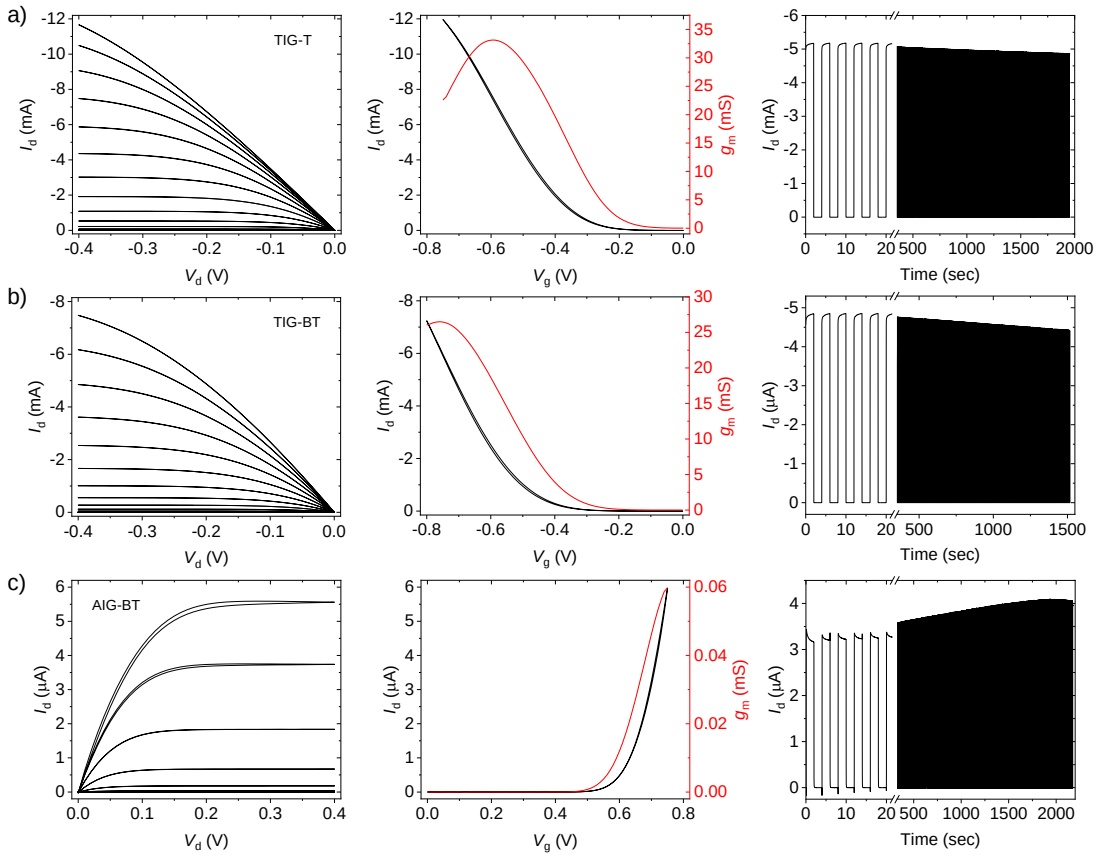

Figure 4. Output (left), transfer and transconductance (middle) and cycling stability (right) plots for OECTs with **TIG-T** (a), **TIG-BT** (b) and **AIG-BT** (c) active materials. OECT channel dimensions 10 × 100 μm (L×W). Output curves at 50 mV gate potential steps, at a sweep rate of 0.2 (**TIG-T** and **TIG-BT**) or 0.05 V_d s^{-1} (**AIG-BT**); transfer curves recorded with V_d of −0.4 V for p-type (**TIG-T** and **TIG-BT**) and 0.4 V for n-type (**AIG-BT**), at a sweep rate of 0.2 or 0.05 V_g s^{-1}; cycling stability recorded with V_g of −0.5 V for **TIG-T**, -0.7 V for **TIG-BT**, and 0.7 V for **AIG-BT**.

Table 1. Summary of OECT Characteristics for the Isoindigo-Derived Polymers

Polymer [units][a)]	OECT operation	V_{th} [V]	g_m [S cm^{-1}][a)]	C^* [F cm^{-3}][b)]	μ_{OECT} [cm^2 V^{-1} s^{-1}][c)]	μC^* [F cm^{-1} V^{-1} s^{-1}][d)]
IG-T	p-type	-0.69	0.023 ± 0.004	76.2 ± 6.9	2.7 10^{-3} ± 5 10^{-4}	0.20 ± 0.03
TIG-T	p-type	-0.20	52 ± 10	121 ± 12	1.1 ± 0.2	132 ± 26
TIG-BT	p-type	-0.34	23 ± 10	82.1 ± 7.9	0.61 ± 0.3	55 ± 28
AIG-BT	n-type	0.55	0.029 ± 0.006	83.5 ± 8.5	1.4 10^{-3} ± 4 10^{-4}	0.12 ± 0.03

[a)]Transconductance values measured at V_g values of -0.8 V (**IG-T**), -0.6 V (**TIG-T**), -0.75 V (**TIG-BT**), and 0.75 V (**AIG-BT**); values normalized by active layer dimensions Wd/L; [b)] Values extracted from electrochemical impedance spectroscopy measurements; [c)] Values extracted from the transistor characteristics in the saturated regime; [d)] Values calculated from the slope of g_m as a function of $(Wd/L)(V_{th} - V_g)$. Average values were extracted from either 5 or 6 measured devices.

Following OECT evaluation, electrochemical impedance spectroscopy was employed to understand the charge capacity of the isoindigo-derived polymers as detailed in the Supporting Information (Figure S23 and S24). The volumetric capacitance C^* was extracted for the four polymers (Table 1) with **IG-T**, **TIG-BT**, and **AIG-BT** all affording comparable values around 80 F cm^{-3} while the value for **TIG-T** was approximately 50% higher at 121 F cm^{-3}. The other material-dependent factor that affects the OECT performance is the electronic charge carrier mobility μ. Extracted from the OECT characteristics in the saturated regime, we observed relatively high hole mobilities of 1.1 cm^2/Vs and 0.61 cm^2/Vs for the two planar thienoisoindigo-based polymers, **TIG-T** and **TIG-BT**, whereas **IG-T** predicted to have a less coplanar backbone showed a much inferior hole mobility around $3 \cdot 10^{-3}$ cm^2/Vs. The n-type material **AIG-BT** had an electron mobility of $1.4 \cdot 10^{-3}$ cm^2/Vs, comparable to the few existing n-type mixed conductors in literature.[15,17,37] The uC^* product takes into account both material-dependent factors of OMIECs and is thus considered an important figure-of-merit for this class of materials.[13] With both the higher volumetric capacitance and superior hole mobility, **TIG-T** naturally displays the highest uC^* of 132 F cm^{-1} V^{-1} s^{-1} which is comparable to other high-performing p-type OMIECs such as the glycolated polythiophene p(g2T-T),[8,13] although better performing materials have been developed recently through judicious optimization of chemical structure and control of microstructure.[7,14] The lower charge carrier mobility and volumetric capacitance of **TIG-BT** is reflected in a uC^* of 55 F cm^{-1} V^{-1} s^{-1} while **IG-T** has a rather low uC^* product of 0.2 F cm^{-1} V^{-1} s^{-1} mainly owing to the poor hole mobility observed for this system. Electron-transporting OMIECs generally show much inferior uC^* values relative to their p-type counterparts due to much poorer charge transport observed for n-type operation at an aqueous interface. This is also seen in this case with **AIG-BT** having a uC^* value of 0.12 F cm^{-1} V^{-1} s^{-1} which is comparable to or better than the glycolated naphthalenediimide-based systems,[13,15,16] but lagging slightly behind some of the subsequent n-type OMIECs that have been developed recently.[17,37,38]

2.4. Computational Simulations

Properties of the polymer series discussed above were examined through a series of density functional theory (DFT) calculations to help explain the observed trends in experimental data. Torsional angle ϕ_2 was varied to generate potential energy surfaces (PES) for rotation around these bonds (Figure 5). These PES confirm the near planar geometries for the AIG polymers and greater twisting for the IG polymers, as inferred from our earlier instinctive consideration of intramolecular interactions along the polymer (Figure 1). The curves also provide an insight into the preference for one conformation over another, for example **AIG-BT** is likely to have the highest degree of conformational uniformity due to the 180° conformer being much more stable than the alternative (ϕ_2 = 30°), with the barrier for rotation also being lower for the rotation from 30° to 180°. While polymers like **AIG-T** have planar minima in both conformations, their energies differ by only 1 kcal/mol with similar barrier heights to rotation. Thus, more disorder might be expected along the polymer chain although planarity is enforced for both possible conformers.

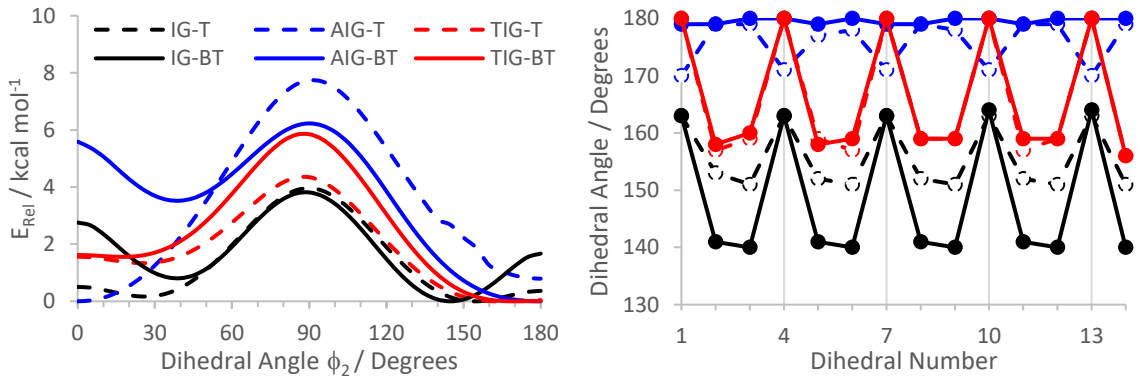

Figure 5. Left. Torsional PES for model repeat unit rotating around ϕ_1. Right. Dihedral angles along optimized polymer chains, where vertical lines highlight intra-isoindigo dihedrals, ϕ_1.

Using the most favorable conformations, oligomers of five repeat units were constructed to represent polymer structures, and the geometries optimized (ωB97XD/6-31G*). Dihedral angles between isoindigo and thiophene/benzothiadiazole groups mirrored the minima from the torsional PES; AIG polymers exhibited planar ϕ_2 dihedrals, TIG polymers possessed a 20° rotation, while the IG polymers were further twisted as seen in Figure 5 (right). For the most

part, internal isoindigo-like torsions, ϕ_1, were independent of the choice of T/BT unit, except for **AIG-T** which exhibited a 10° twist relative to **AIG-BT**.

Electronic properties were investigated through the use of a tuned range separated functional approach (Table 2). Optimal omega values were smallest for the two TIG polymers, indicating a greater degree of electronic delocalization, with the IG polymers also having similar values to one another. The comonomer was more influential in the AIG polymers, where a smaller ω value indicated more delocalization in **AIG-BT** than in **AIG-T** in agreement with the slightly increased backbone planarity for the BT polymer. Hence, both electronic and geometric factors contribute to the degree of delocalization.

Table 2. Computed electronic properties of polymer series.

	Optimal ω / $Bohr^{-1}$ [a]	IP / eV [b]	EA / eV [b]	P^+ IG% [b),c]	P^- IG% [b),c]
IG-T	0.1128	5.66	2.75	68	87
IG-BT	0.1126	5.88	2.74	79	83
AIG-T	0.1249	5.77	2.96	66	85
AIG-BT	0.1074	6.00	3.02	67	77
TIG-T	0.0834	4.92	2.80	75	81
TIG-BT	0.0781	5.02	2.98	77	65

[a] ωB97XD/6-31G* in gas phase, [b] optimized ωB97XD/6-31G* in chloroform polarizable continuum, c) percent of charge stabilized on the isoindigo fragments in positively (P^+) or negatively (P^-) charged systems, analyzed by Hirshfeld atomic charges.

Using the optimally tuned functionals, ionization potential (IP) and electron affinity (EA) energies were calculated as the difference in single point energies of the charged and neutral species. IP energies follow a general trend of TIG<IG<AIG, where the electron-deficient BT comonomer increases the IP relative to the more electron-rich thiophene by 0.1-0.2 eV. These trends are broadly in line with the experimental data (Table S1) including also the (spectro)electrochemistry and OECT devices, where **TIG-T** shows the smallest magnitudes for oxidation or p-type threshold voltage although the effect of BT versus thiophene comonomer on IP values is slightly underestimated computationally. The trend in EA is IG<TIG<AIG with less of an influence from the BT or T comonomers. Again, we find a reasonable match between predicted and measured values; yet, the two TIG polymers are

found experimentally to have markedly lower electron affinities than their AIG counterparts by roughly 0.3-0.4 eV.

The distributions of both positive and negative polarons (P^+ and P^-) were calculated by dividing the polymer into fragments and running Hirshfeld charge calculations. Since the isoindigo type groups are much larger than either BT or T, they were split into two fragments for a more fair comparison. In positively charged systems, TIG polymers bear most of their excess charge on the TIG groups, while AIG provides less stabilization for the charge. A more delicate balance in electronics is observed in the IG polymers, where the nature of the BT/T group results in changes to the charge stabilization on these units.

In general, the isoindigoid motifs bear more localized charge in the negatively charged polymers than the positive ones. Despite having little influence on EA energies, the BT group serves to stabilize negative charge more than T throughout the polymer series, while there is an increased charge percentage on the IG groups in the order TIG<AIG<IG.

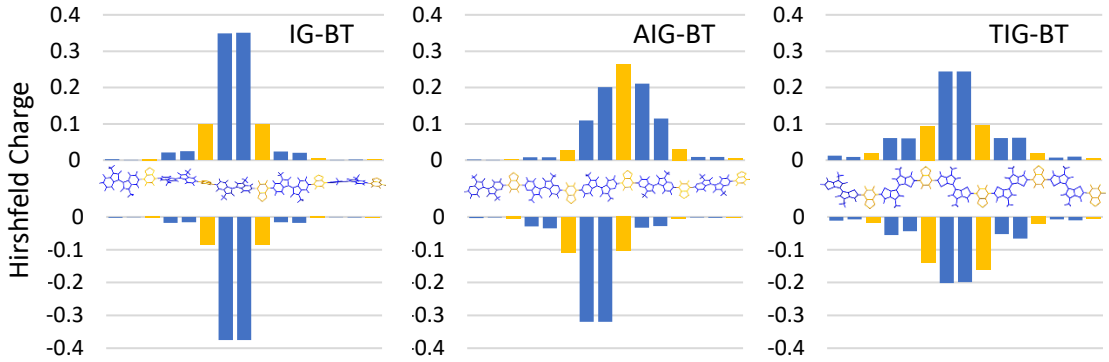

Figure 6. Hirshfeld charge distribution by fragment (Blue = isoindigo-type, Yellow = BT) for BT containing polymers. P^+ shown as positive bars and P^- shown as negative bars. Each IG-type monomer is split into two parts for comparison.

As well as the overall percentage stabilizations, there are clear differences in charge distribution along the polymer chains as visualized for the BT copolymers in Figure 6. For P^+ states, **IG-BT** shows the most localization, with nearly 70 % of the charge on a single IG unit in the middle of the chain. **AIG-BT** exhibits its greatest positive charge residing on a central

BT unit, and spreading over the two adjacent AIG groups. **IG-T** and **AIG-T** show similar distributions to **AIG-BT** (Figure S25). TIG polymers show much more delocalization, in part due to their relatively planar structures, but also influenced by the lower aromaticity of thiophene versus the pyridine or benzene rings found in AIG and IG. For P^-, most of the polymers show greatest localization on an isoindigo group, but with differing amounts of charge spreading to other parts of the chain. Of these, **AIG-BT** seems to show greater delocalization than the other IG and AIG polymers, while the TIG polymers once again exhibit a greater degree of delocalization. These results would suggest that the two TIG polymers should perform better as both n- and p-type semiconductors, although only p-type operation is observed experimentally.

Our computational analysis points towards a couple of design principles which might be used in future organic semiconductor polymer synthesis. The first is that both TIG polymers show large degrees of electronic delocalization in comparison to the other isoindigo groups, and should be considered with other co-monomers in future polymers. Further computational study of polymers containing this group is underway to determine whether geometric or electronic effects are the main cause of the extended polaron delocalization. A second design feature for consideration is the role of both of the co-monomers within the polymer chain, affecting the planarity and conformational uniformity of the polymer as well as charge localization along the chain. Careful energetic matching of these sub-units may result in more delocalization and better performing materials. Another consideration is the overall weighting of the different monomers in the copolymer. Here, the isoindigo groups are much larger than thiophene and benzothiadiazole, and so contribute more to the polymer properties. The atom-balance may well prove another important feature in designing new materials as semiconductors in general, and for OECTs in particular.

2.5. Structural Properties

Thin films of each copolymer were characterized via grazing incidence wide-angle x-ray scattering (GIWAXS, Figure 7 and Table 3) to elucidate structural origins of device performance. The copolymers in this series displayed characteristic lamellar (100) and π-stack (010) scattering common to semi-crystalline conjugated polymers at q ~ 0.25-0.33 $Å^{-1}$ and q ~ 1.6-1.8 $Å^{-1}$, respectively, which were broadly in line with previous reports of alkyl and glycol side chain analogues.[26,28,35,39] All copolymer scattering patterns exhibited populations of both face-on (out-of-plane π-stack) and edge-on (in-plane π-stack) crystallites, with T containing copolymers favoring larger populations of face-on and BT copolymers favoring larger populations of edge-on crystallites. IG and AIG based copolymers were more susceptible to preferentially stacking either face- or edge-on when polymerized with T or BT, respectively, whereas TIG based copolymers exhibited more equal populations of both. Line-cuts highlight the relative strength of in- and out-of-plane lamellar (h00) and π-stack (010) scattering (Figure 8). All three BT polymers showed an in-plane peak between 1.2 and 1.4 $Å^{-1}$, which we tentatively attributed to ordering of the glycol containing side chains as they were not an integer multiple of any other peaks present and yielded similar d-spacing that would be expected from the packing of oligoethylene glycol helices.[40,41]

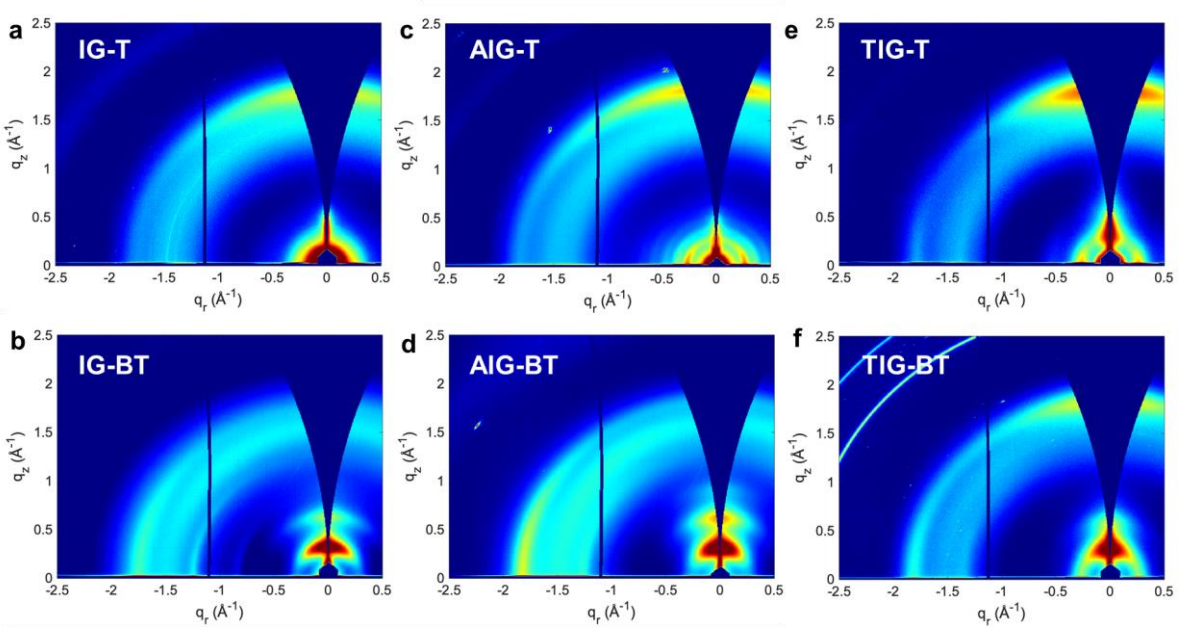

Figure 7. 2-D GIWAXS patterns of (a) IG-T, (b) IG-BT, (c) AIG-T, (d) AIG-BT, (e) TIG-T, (f) TIG-BT showing preferential face-on stacking for thiophene (T) copolymers and preferential edge-on stacking for benzothiadiazole (BT) copolymers.

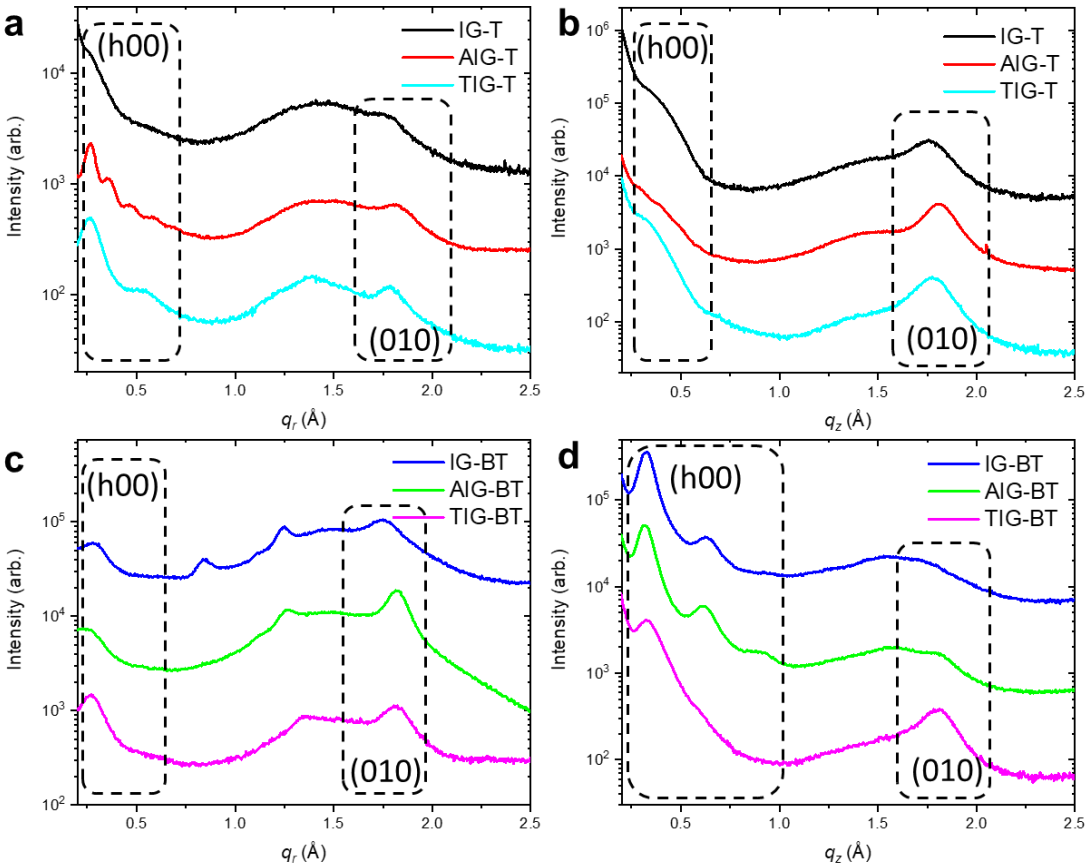

Figure 8. GIWAXS Line-cuts. In-plane (q_r) and out-of-plane (q_z) line cuts of thiophene copolymers, (a) and (c), and benzothiadiazole copolymers, (b) and (d), respectively. Lamellar (h00) and π peaks (010) labeled accordingly.

Beyond the above-mentioned preferential face-on nature of **IG-BT** and edge-on nature of **IG-T, IG-T** exhibited relatively weak lamellar ordering manifested as broad scattering shoulders with no higher order peaks. Additionally, **IG-BT** displayed a scattering peak at 0.84 $Å^{-1}$, representing a d-spacing of 7.45 Å, which is approximately half the length of the copolymer repeat unit (~14.6 Å). This potentially indicated that the chains are stacked with an alternating cofacial alignment between copolymer backbones, similar to the copolymers investigated by Brinkmann et. al. [42] The diminished planarity, large periodic fluctuations in dihedral angle,

and high degree of localization of electron density on the isoindigo repeat units (all assessed through calculations) may all contribute to the preferential cofacial alignment of IG with BT units in the π-stack. The π-stack d-spacings of these copolymers (3.59 and 3.57 Å for **IG-BT** and **IG-T**, respectively), with alkyl spacers offsetting the oligoethylene glycol units on the side chains, were tighter than previous reports of **IG-T** analogues with branched oligoethylene glycol (3.64 Å) or branched alkyl (3.76 Å) sidechains.[39]

Table 3. GIWAXS in-plane and out-of-plane d-spacing in lamellar and π stacking directions with corresponding coherence lengths.

Polymer	In-plane				Out-of-plane			
	d_{100} (Å)	$L_{c,100}$ (Å)	d_{010} (Å)	$L_{c,010}$ (Å)	d_{100} (Å)	$L_{c,100}$ (Å)	d_{010} (Å)	$L_{c,010}$ (Å)
IG-T	23.7*	--	3.5*	--	17.1*	--	3.57	35.6
IG-BT	22.4	40.4	3.59	25.6	19.3	69.1	4.0*	--
AIG-T	23.7 (35.1**)	92.8	3.4*	--	18.5*	--	3.47	39.2
AIG-BT	24.5	42.9	3.45	53.4	19.7	74.8	3.5*	--
TIG-T	23.7	55.8	3.52	36.0	19.5*	--	3.54	33.6
TIG-BT	23.7	43.1	3.45	41.6	18.8	41.7	3.48	32.6

* Peaks present but not well resolved indicating that exact values are inaccurate.
** Polymorph q_r

AIG-T and **AIG-BT** both displayed multiple orders of (h00) scattering peaks, indicating significant lamellar ordering. Interestingly, **AIG-T** presented two conflated series of low-q peaks, suggesting the presence of two distinct polymorphs with different lamellar spacings, a predominant polymorph with a d_{100} of 23.7 Å and a minor population with $d_{1'00}$ of 35.1 Å. **AIG-BT**, which was predicted to be the most planar, has three orders of nicely resolved lamellae scattering and a larger out-of-plane coherence length than any of the other polymers. Both AIG polymers had similar d_{010} around 3.45 Å, which was tighter than previously

reported selenophene containing analogues with branched alkyl side chains (d_{010} of 3.67 Å).[28]

Both TIG copolymers showed similar scattering patterns with comparable lamellar spacing, though **TIG-T** presented stronger in-plane lamellar ordering, apparent from the presence of a second order scattering peak, while **TIG-BT** displayed stronger out-of-plane lamellar ordering, apparent as a well-defined scattering peak compared to the shoulder in **TIG-T**. **TIG-BT** displayed a tighter in-plane d_{010} (3.45 Å) and longer coherence length. This π-stack spacing is also smaller than previously reported for a **TIG-BT** polymer with branched alkyl sidechains (3.6 Å).[26]

Connecting these copolymer structures to OECT performance, the top performing copolymers (**TIG-T** and **TIG-BT**) both had populations of edge-on and face-on crystallites with significant π-stacking in- and out-of-plane. Presuming that intermolecular charge transport is enhanced in the direction of π-stacking, improved OECT performance is to be expected as charging and charge transport in OECT channels is not interfacial, but volumetric, with charge transport progressing through three dimensional percolative pathways. The lack of significant differences between **TIG-T** and **TIG-BT** microstructure indicates that the difference in hole mobility may be due to the difference in ionization potential (4.5 eV and 4.8 eV, respectively) as well as the slightly more extended delocalization of positive charge beyond the TIG unit for **TIG-T** as observed computationally (Table 2). **IG-T**, in comparison, had much lower hole mobilities, likely due to its relative lack of chain ordering (especially diminished lamellar stacking and in-plane π-stacking) and large IP energy. With the presence of apparent ordering in the backbone direction of **IG-BT** one might reasonably expect improved charge transport, however any OECT channel conductance was precluded by the prohibitively large IP.

3. Discussion and Conclusion

Three different isoindigoid motifs with amphipathic side chains comprising a five methylene spacer and a triethylene glycol moiety were synthesized and copolymerized with the electron-rich thiophene (T) comonomer and the electron-deficient 2,1,3-benzothiadiazole (BT) comonomer. The frontier energy levels of the polymers are mainly governed by the choice of isoindigoid moiety and less so by the nature of the comonomer unit with thienoisoindigo (TIG) based polymers displaying very narrow optical band gaps, low IPs in the range 4.5-4.8 eV and relatively high EAs (3.6-3.9 eV) making them in principle candidates for both p- and n-type operation in aqueous media. A strong electronic delocalization is observed in the TIG polymers, which we ascribe to a planar polymer backbone and the relatively low aromaticity of thiophene favoring contributions from a quinoidal-like resonance form. The parent isoindigo (IG) and 7,7'-diazaisoindigo (AIG), comprising more aromatic benzene and pyridine moieties, afford significantly wider band gap polymers with restrictively large IP values in the range 5.3-5.9 eV, too large for stable p-type operation in aqueous electrolyte considering the limited electrochemical window of water. Relatively large EA values, on the other hand, in particular for the electron-deficient pyridine derivative copolymerized with the electron-deficient BT comonomer (4.2 eV), pave the way for facile electron injection and potential n-type operation in aqueous media. Although the IG and AIG polymers display lower degrees of electronic delocalization than the TIG polymers, owing to their higher degree of aromaticity, we note that good polaronic charge distribution along the polymer backbone is predicted computationally for the AIG polymers with both the isoindigoid and the comonomer unit accommodating the polaronic charge. This is most likely a result of the highly planar backbone conformation for the AIG polymers, something that is not observed for the IG polymers where steric hindrance between adjacent polymer backbone units causes significant twisting.

Corroborating the observed trends relating to the frontier energy levels, we find that the two TIG polymers with relatively low IPs undergo reversible oxidative electrochemical switching

in the solid state in aqueous electrolyte, while the corresponding spectroelectrochemical studies confirm that the bulk of the neutral polymer film bleaches in this manner with concurrent formation of stable positive polarons for both **TIG-T** and **TIG-BT**. Even though some reductive behavior was observed for the two TIG polymers in CV, as one could also expect in particularly for **TIG-BT** due to its relatively high EA of 3.9 eV, spectroelectrochemical studies did not show evidence of effective bleaching of the bulk polymer films under these conditions with only a very small decrease of the neutral absorption bands observed for both polymers even at 1.2 V applied potential. Isoindigo polymer **IG-T** likewise shows oxidative behavior even though a much higher onset of oxidation confirms the larger IP compared to the TIG polymers. The AIG polymers afford much lower current densities in the CV experiments than the TIG polymers and no clear Faradaic-like redox events are observed although **AIG-BT** does show a more capacitive-like current response, particularly upon electrochemical reduction. Spectroelectrochemistry confirms that reduction of the **AIG-BT** film does indeed take place with concurrent formation of negative polaronic species that are stable in aqueous electrolyte. Oxidation of **AIG-BT**, on the other hand, does not produce a spectroelectrochemical response, in agreement with the large IP value of 5.9 eV discussed above.

Interestingly, we find that the two thiophene copolymers (**IG-T** and **TIG-T**) undergo their spectroelectrochemical bleaching process rapidly within an electrochemical potential window of approximately 0.3 V while the two BT copolymers (**AIG-BT** and **TIG-BT**) bleach much more gradually over approximately an 0.8 V potential range. To that effect, we note that GIWAXS analysis clearly showed that the thiophene copolymers had a predominant face-on texture while the BT copolymers had a higher population of edge-on crystallites. Although previous studies have focused on chemical doping, there is literature precedent indicating that surface-doping is facilitated by face-on oriented polymer domains.[43]

Electrochemical and spectroelectrochemical studies in aqueous electrolyte serve as an excellent initial screening tool for active materials for OECT applications and we do indeed find that **IG-T**, **TIG-T** and **TIG-BT**, who all displayed good oxidative electrochromic behavior, can be employed as p-type mixed conductors in a conventional OECT configuration interfaced with aqueous sodium chloride solution. The relatively poor performance of **IG-T**, with a high threshold voltage of -0.69 V, a normalized transconductance of 23 mS cm^{-1} and a μC* product of 0.20 F cm^{-1} V^{-1} s^{-1}, is to be expected considering the low degree of backbone planarity, relatively weak structural ordering observed by GIWAXS and consequently a low hole mobility on the order of 10^{-3} cm^2/Vs. The TIG chromophore, on the other hand, furnishes low band gap polymers with better electronic delocalization along the polymer backbone, a more coplanar geometry and a lower IP, which is manifested in high-performing p-type OECT devices for both **TIG-T** and **TIG-BT**. The slightly more electron-rich **TIG-T** provides a lower threshold voltage (-0.20 V *vs.* -0.34 V for **TIG-BT**), a high normalized transconductance of 52 S cm^{-1} (compared to 23 S cm^{-1} for **TIG-BT**) and a μC* product of 132 F cm^{-1} V^{-1} s^{-1}. Good charge transport properties with extracted hole mobilities around 1.1 cm^2/Vs for **TIG-T** and 0.6 cm^2/Vs for **TIG-BT** are ascribed to strong electronic delocalization and a very good distribution of polaronic charge over the entire polymer backbone as well as close π-stacking distances and relatively long crystallite coherence lengths. The subtle structural modification of changing the isoindigoid scaffold from thienoisoindigo to 7,7'-diazaisoindigo has pronounced impact on structural and electronic properties. Going from **TIG-BT** to **AIG-BT** sees the EA value increase from 3.9 eV to 4.2 eV; hence, **AIG-BT** shows promising n-type OECT behavior with a threshold voltage of 0.55 V, a normalized transconductance of 29 mS cm^{-1} and a μC* product of 0.12 F cm^{-1} V^{-1} s^{-1}. **AIG-BT** stands out among all the polymers discussed herein not only by the largest EA but also by having a particularly coplanar structure which in turn allows for strong interchain interactions reflected in extraordinarily tight π-stacking (3.45 Å) and a very large in-plane

coherence length corresponding to more than 15 polymer chains in the average π-stack. Coupled with good electron delocalization and efficient negative charge distribution across the entire polymer backbone, these appear to be the governing factors for efficient n-type OECT behavior across this series of polymers. Despite promising characteristics for n-type OECT operation, such as relatively high EA values and efficient stabilization of negative polaronic charges along the polymer backbone, neither **TIG-T** nor **TIG-BT** showed significant reductive electrochromic behavior or n-type mixed conduction properties in OECTs. As stated above, it appears that the much enhanced conformational planarity and uniformity of **AIG-BT**, with one coplanar backbone conformation being heavily favored, is a crucial factor for stable n-type operation in an aqueous environment. As such, **TIG-T** and **TIG-BT** are found to be much more structurally flexible with smaller barriers for rotation and less energetic difference between the possible conformers.

From GIWAXS analysis, we observe that all six polymers show close π-stacking distances in the range 3.4-3.5 Å, shorter than other closely related derivatives reported in literature, indicating that the linear amphipathic side chain not only facilitates ionic transport across an aqueous interface but also efficient intermolecular interactions.[25] Glycolated polythiophenes generally orient edge-on relative to the substrate,[8,14] whereas this polymer series provides examples of both face-on and edge-on textured systems with good OECT performance. Although there might be important subtleties setting the different orientations apart, as noticed here for the electrochromic bleaching which is abrupt over a short potential range for the thiophene copolymers and more gradual for the BT copolymers, it is clear that future molecular design needs not focus exclusively on e.g. edge-on oriented systems. Furthermore, as additional comonomers beyond thiophene and 2,1,3-benzothiadiazole are explored for these isoindigoid motifs, a better understanding of the structure-property relations that govern the polymer orientation will be achievable.

Considering general design criteria and future work that might be extrapolated from this study, TIG stands out as an excellent building block for future p-type OMIECs due to a suitably low IP, a strong electronic delocalization along the polymer backbone, and efficient stabilization of polaronic charges. Exploration of other comonomers beyond T and BT could shed light on the role of energetic matching of comonomer units and how it can be used as a molecular design tool for further enhancing the favorable electronic properties observed for **TIG-T** and **TIG-BT**. Given the very low band gap of TIG-based polymers, the scope for ambipolar mixed conduction with this moiety should not be overlooked. Our computational studies indicate a very good ability for negative polaronic charges to be accommodated along the polymer backbone, in particular for **TIG-BT**. Although this was not reflected in the OECT performance, with no n-type behavior observed, we anticipate that derivatives with slightly larger EA values and a higher degree of conformational rigidity could emerge as promising ambipolar mixed conductors. The more electron-deficient AIG moiety likewise emerges as a promising building block, in particular for n-type OMIECs owing to a relatively high EA, good electronic delocalization, and a highly coplanar geometry with strong conformational uniformity which facilitates strong π-stacking interactions over extended length scales. We note that this structural rigidity is also found in other high-performing n-type OMIECs such as the ladder-type polymer BBL and the double-bond-linked condensation polymer PgNaN.[17,37] As conformational uniformity and rigidity is starting to appear as a more general design criteria for n-type OMIECs, AIG-based systems provide a good platform for exploring this further for instance with new comonomers providing so-called conformational locking by taking advantage of noncovalent interactions.[44,45] In this context, the computational studies also clearly show that the choice of comonomer has a rather large effect on the negative polaronic charge distribution with BT facilitating a significantly better charge delocalization across the entire polymer backbone than for instance the thiophene comonomer. Interestingly, much less of a direct interplay between choice of comonomer and

positive polaronic charge distribution is observed and we notice that these trends are equally valid for both TIG and AIG motifs.

In conclusion, we have identified a highly modular semiconducting polymer system that not only provides good p- and n-type OMIECs but also lends itself very nicely to further structural exploration. Our work, synergistically combining molecular design, spectro-electrochemical studies, OECT device evaluation, structural analysis and computational investigations, has identified 7,7'-diazaisoindigo (AIG) as a promising building block for n-type OMIECs while thienoisoindigo (TIG) affords p-type OMIECs and also holds the potential for furnishing ambipolar OMIECs with further optimisation.

Supporting Information

Supporting Information is available from the Wiley Online Library or from the author.

Acknowledgements

Z.S.P., J.B.G., and C.B.N. gratefully acknowledge support from the Academy of Medical Sciences & Wellcome Trust (SBF002/1158) and the Materials Research Institute. B.D.P. and J.R. gratefully acknowledge support from the National Science Foundation grant no. NSF DMR-1751308. This research used resources of the Advanced Photon Source (beamline 8-ID-E), a U.S. Department of Energy (DOE) Office of Science User Facility operated for the DOE Office of Science by Argonne National Laboratory under Contract No. DE-AC02-06CH11357. This work utilized Northwestern University Micro/Nano Fabrication Facility (NUFAB), which is partially supported by Soft and Hybrid Nanotechnology Experimental (SHyNE) Resource (NSF ECCS-1542205), the Materials Research Science and Engineering Center (DMR-1720139), the State of Illinois, and Northwestern University. This work made use of the Keck-II and EPIC facilities of Northwestern University's NU*ANCE* Center, which has received support from the Soft and Hybrid Nanotechnology Experimental (SHyNE) Resource (NSF ECCS-1542205); the MRSEC program (NSF DMR-1720139) at the Materials Research Center; the International Institute for Nanotechnology (IIN); the Keck Foundation; and the State of Illinois, through the IIN.

Received: ((will be filled in by the editorial staff))
Revised: ((will be filled in by the editorial staff))
Published online: ((will be filled in by the editorial staff))

References

[1] M. Berggren, A. Richter-Dahlfors, *Adv. Mater.* **2007**, *19*, 3201.

[2] T. Someya, Z. Bao, G. G. Malliaras, *Nature* **2016**, *540*, 379.

[3] B. D. Paulsen, K. Tybrandt, E. Stavrinidou, J. Rivnay, *Nat. Mater.* **2020**, *19*, 13.

[4] J. Rivnay, P. Leleux, M. Sessolo, D. Khodagholy, T. Hervé, M. Fiocchi, G. G. Malliaras, *Adv. Mater.* **2013**, *25*, 7010.

[5] S. T. Keene, T. P. A. van der Pol, D. Zakhidov, C. H. L. Weijtens, R. A. J. Janssen, A. Salleo, Y. van de Burgt, *Adv. Mater.* **2020**, *32*, 2000270.

[6] P. Jastrzebska-Perfect, G. D. Spyropoulos, C. Cea, Z. Zhao, O. J. Rauhala, A. Viswanathan, S. A. Sheth, J. N. Gelinas, D. Khodagholy, *Sci. Adv.* **2020**, *6*, eaaz6767.

[7] Y. Kim, H. Noh, B. D. Paulsen, J. Kim, I. Y. Jo, H. J. Ahn, J. Rivnay, M. H. Yoon, *Adv. Mater.* **2021**, *33*, 2007550.

[8] C. B. Nielsen, A. Giovannitti, D.-T. T. Sbircea, E. Bandiello, M. R. Niazi, D. A. Hanifi, M. Sessolo, A. Amassian, G. G. Malliaras, J. Rivnay, I. Mcculloch, *J. Am. Chem. Soc.* **2016**, *138*, 10252.

[9] A. Giovannitti, D.-T. Sbircea, S. Inal, C. B. Nielsen, E. Bandiello, D. A. Hanifi, M. Sessolo, G. G. Malliaras, I. McCulloch, J. Rivnay, *Proc. Natl. Acad. Sci.* **2016**, *113*, 12017.

[10] E. Zeglio, J. Eriksson, R. Gabrielsson, N. Solin, O. Inganäs, *Adv. Mater.* **2017**, *29*, 1605787.

[11] T. Nicolini, J. Surgailis, A. Savva, A. D. Scaccabarozzi, R. Nakar, D. Thuau, G. Wantz, L. J. Richter, O. Dautel, G. Hadziioannou, N. Stingelin, *Adv. Mater.* **2020**, *33*, 2005723.

[12] M. Moser, A. Savva, K. Thorley, B. D. Paulsen, T. C. Hidalgo, D. Ohayon, H. Chen, A. Giovannitti, A. Marks, N. Gasparini, A. Wadsworth, J. Rivnay, S. Inal, I. McCulloch, *Angew. Chemie* **2021**, *133*, 7856.

[13] S. Inal, G. G. Malliaras, J. Rivnay, *Nat. Commun.* **2017**, *8*, 1767.

[14] M. Moser, T. C. Hidalgo, J. Surgailis, J. Gladisch, S. Ghosh, R. Sheelamanthula, Q. Thiburce, A. Giovannitti, A. Salleo, N. Gasparini, A. Wadsworth, I. Zozoulenko, M. Berggren, E. Stavrinidou, S. Inal, I. McCulloch, *Adv. Mater.* **2020**, *32*, 2002748.

[15] A. Giovannitti, C. B. Nielsen, D.-T. T. Sbircea, S. Inal, M. Donahue, M. R. Niazi, D. A. Hanifi, A. Amassian, G. G. Malliaras, J. Rivnay, I. Mcculloch, *Nat. Commun.* **2016**, *7*, 13066.

[16] A. Giovannitti, I. P. Maria, D. Hanifi, M. J. Donahue, D. Bryant, K. J. Barth, B. E. Makdah, A. Savva, D. Moia, M. Zetek, P. R. F. Barnes, O. G. Reid, S. Inal, G. Rumbles, G. G. Malliaras, J. Nelson, J. Rivnay, I. McCulloch, *Chem. Mater.* **2018**, *30*, 2945.

[17] H. Sun, M. Vagin, S. Wang, X. Crispin, R. Forchheimer, M. Berggren, S. Fabiano, *Adv. Mater.* **2018**, *30*, 1704916.

[18] C. G. Bischak, L. Q. Flagg, K. Yan, C. Z. Li, D. S. Ginger, *ACS Appl. Mater. Interfaces* **2019**, *11*, 28138.

[19] J. Surgailis, A. Savva, V. Druet, B. D. Paulsen, R. Wu, A. Hamidi-Sakr, D. Ohayon, G. Nikiforidis, X. Chen, I. McCulloch, J. Rivnay, S. Inal, *Adv. Funct. Mater.* **2021**, *31*, 2010165.

[20] Z. S. Parr, R. Halaksa, P. A. Finn, R. B. Rashid, A. Kovalenko, M. Weiter, J. Rivnay, J. Krajčovič, C. B. Nielsen, *Chempluschem* **2019**, *84*, 1384.

[21] Z. S. Parr, R. B. Rashid, B. D. Paulsen, B. Poggi, E. Tan, M. Freeley, M. Palma, I. Abrahams, J. Rivnay, C. B. Nielsen, *Adv. Electron. Mater.* **2020**, *6*, 2000215.

[22] X. Wu, Q. Liu, A. Surendran, S. E. Bottle, P. Sonar, W. L. Leong, *Adv. Electron. Mater.* **2021**, *7*, 2000701.

[23] H. Jia, Z. Huang, P. Li, S. Zhang, Y. Wang, J. Y. Wang, X. Gu, T. Lei, *J. Mater. Chem. C* **2021**, *9*, 4927.

[24] G. Krauss, F. Meichsner, A. Hochgesang, J. Mohanraj, S. Salehi, P. Schmode, M. Thelakkat, *Adv. Funct. Mater.* **2021**, *31*, 2010048.

[25] Y. Wang, E. Zeglio, H. Liao, J. Xu, F. Liu, Z. Li, I. P. Maria, D. Mawad, A. Herland, I. Mcculloch, W. Yue, *Chem. Mater.* **2019**, *31*, 9797.

[26] R. S. Ashraf, A. J. Kronemeijer, D. I. James, H. Sirringhaus, I. McCulloch, *Chem. Commun.* **2012**, *48*, 3939.

[27] R. Stalder, J. Mei, K. R. Graham, L. A. Estrada, J. R. Reynolds, *Chem. Mater.* **2014**, *26*, 664.

[28] W. Yue, M. Nikolka, M. Xiao, A. Sadhanala, C. B. Nielsen, A. J. P. White, H.-Y. Chen, A. Onwubiko, H. Sirringhaus, I. McCulloch, *J. Mater. Chem. C* **2016**, *4*, 9704.

[29] Y. K. Voronina, D. B. Krivolapov, A. V Bogdanov, V. F. Mironov, I. A. Litvinov, *J. Struct. Chem.* **2012**, *53*, 413.

[30] J. Huang, Z. Mao, Z. Chen, D. Gao, C. Wei, W. Zhang, G. Yu, *Chem. Mater.* **2016**, *28*, 2209.

[31] J. Liu, G. Ye, H. G. O. Potgieser, M. Koopmans, S. Sami, M. I. Nugraha, D. R. Villalva, H. Sun, J. Dong, X. Yang, X. Qiu, C. Yao, G. Portale, S. Fabiano, T. D. Anthopoulos, D. Baran, R. W. A. Havenith, R. C. Chiechi, L. J. A. Koster, *Adv. Mater.* **2021**, *33*, 2006694.

[32] J. Mei, K. R. Graham, R. Stalder, J. R. Reynolds, *Org. Lett.* **2010**, *12*, 660.

[33] M. Ashizawa, T. Hasegawa, S. Kawauchi, H. Masunaga, T. Hikima, H. Sato, H. Matsumoto, *RSC Adv.* **2016**, *6*, 109434.

[34] D. Yoo, T. Hasegawa, M. Ashizawa, T. Kawamoto, H. Masunaga, T. Hikima, H. Matsumoto, T. Mori, *J. Mater. Chem. C* **2017**, *5*, 2509.

[35] G. Kim, A. R. Han, H. R. Lee, J. Lee, J. H. Oh, C. Yang, *Chem. Commun.* **2014**, *50*, 2180.

[36] N. M. Randell, C. L. Radford, J. Yang, J. Quinn, D. Hou, Y. Li, T. L. Kelly, *Chem.*

Mater. **2018**, *30*, 4864.

[37] X. Chen, A. Marks, B. D. Paulsen, R. Wu, R. B. Rashid, H. Chen, M. Alsufyani, J. Rivnay, I. McCulloch, *Angew. Chemie - Int. Ed.* **2021**, *60*, 9368.

[38] K. Feng, W. Shan, S. Ma, Z. Wu, J. Chen, H. Guo, B. Liu, J. Wang, B. Li, H. Y. Woo, S. Fabiano, W. Huang, X. Guo, *Angew. Chemie Int. Ed.* **2021**, DOI 10.1002/anie.202109281.

[39] X. Chen, Z. Zhang, J. Liu, L. Wang, *Polym. Chem.* **2017**, *8*, 5496.

[40] A. C. French, A. L. Thompson, B. G. Davis, *Angew. Chemie - Int. Ed.* **2009**, *48*, 1248.

[41] R. K. Hallani, B. D. Paulsen, A. J. Petty, R. Sheelamanthula, M. Moser, K. J. Thorley, W. Sohn, R. B. Rashid, A. Savva, S. Moro, J. P. Parker, O. Drury, M. Alsufyani, M. Neophytou, J. Kosco, S. Inal, G. Costantini, J. Rivnay, I. McCulloch, *J. Am. Chem. Soc.* **2021**, *143*, 11007.

[42] M. Brinkmann, E. Gonthier, S. Bogen, K. Tremel, S. Ludwigs, M. Hufnagel, M. Sommer, *ACS Nano* **2012**, *6*, 10319.

[43] F. Zhang, E. Mohammadi, G. Qu, X. Dai, Y. Diao, *Adv. Mater.* **2020**, *32*, 2002823.

[44] N. E. Jackson, B. M. Savoie, K. L. Kohlstedt, M. Olvera De La Cruz, G. C. Schatz, L. X. Chen, M. A. Ratner, *J. Am. Chem. Soc.* **2013**, *135*, 10475.

[45] K. J. Thorley, I. McCulloch, *J. Mater. Chem. C* **2018**, *6*, 12413.

*Zachary S. Parr, Jorge Borges-González, Reem B. Rashid, Karl J. Thorley, Dilara Meli, Bryan D. Paulsen, Joseph Strzalka, Jonathan Rivnay and Christian B. Nielsen**

From p- to n-Type Mixed Conduction in Isoindigo-Based Polymers through Molecular Design

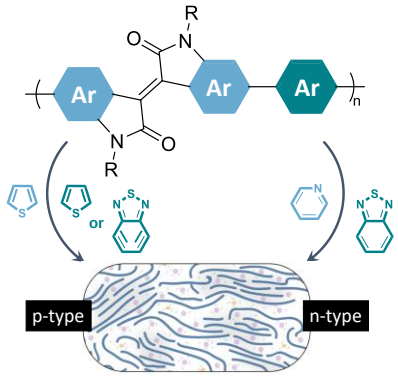

We present new molecular design criteria for isoindigo-based semiconducting polymers and showcase their versatility for the development of mixed conductors relevant to organic bioelectronic applications. Through rational choice of isoindigoid motif and an appropriate comonomer, we develop efficient hole- and electron-transport materials and identify strategies for further optimization including the development of ambipolar mixed conductors.